

## Predicting the vapor-liquid equilibrium of carbon dioxide+alkanol systems by using an artificial neural network

Bahman Zarenezhad<sup>†</sup> and Ali Aminian

School of Chemical, Petroleum and Gas Engineering, Semnan University, P. O. Box 35195-363, Semnan, Iran  
(Received 23 August 2010 • accepted 25 November 2010)

**Abstract**—A multi-layer feed-forward artificial neural network has been presented for accurate prediction of the vapor liquid equilibrium (VLE) of CO<sub>2</sub>+alkanol mixtures. Different types of alkanols namely, 1-propanol, 2-propanol, 1-butanol, 1-pentanol, 2-pentanol, 1-hexanol and 1-heptanol, are used in this study. The proposed network is trained using the Levenberg-Marquardt back propagation algorithm, and the tan-sigmoid activation function is applied to calculate the output values of the neurons of the hidden layers. According to the network's training, validation and testing results, a six layer neural network is selected as the best architecture. The presented model is very accurate over wide ranges of experimental pressure and temperatures. Comparison of the suggested neural network model with the most important thermodynamic correlations shows that the proposed neuromorphic model outperforms the other available alternatives. The predicted equilibrium pressure and vapor phase CO<sub>2</sub> mole fraction are in good agreement with experimental data suggesting the accuracy of the proposed neural network model for process design.

Key words: Artificial Neural Network, Vapor-liquid Equilibrium, Supercritical, CO<sub>2</sub>, Alkanol

### INTRODUCTION

Accurate prediction of vapor-liquid equilibrium is important in the modeling and design of processes that use supercritical fluids for separation processes. The study of CO<sub>2</sub>-alkanol mixtures is of special interest in the extraction of biomolecules with supercritical carbon dioxide, in the extraction of alkanols from aqueous solutions with CO<sub>2</sub> and in the production of n-alkanols from syngas. Super-critical CO<sub>2</sub>, in particular in combination with alkanols, has been identified as an attractive environmentally benign solvent since it is non-toxic, non-flammable, inexpensive and easily recyclable [1,2]. To determine the proper operating conditions for such processes, it is necessary to carry out phase equilibrium calculations over a wide range of pressures and temperatures. Information about the phase behavior of binary mixtures can be obtained from direct measurement of phase equilibrium data or by using thermodynamic models [3]. The capabilities of different thermodynamic models for predicting the phase equilibrium of high pressure asymmetric mixtures containing CO<sub>2</sub> have been investigated [4,5].

Elizalde-Solis et al. [6] studied the phase behavior of binary systems of CO<sub>2</sub>+1-hexanol and CO<sub>2</sub>+1-heptanol by using the Peng-Robinson equation of state (PR EOS) [7] with the Wong-Sandler (WS) mixing rules [8]. Secuijanu et al. [9,10] used the Soave-Redlich-Kwong (SRK) EOS[11] coupled with Huron-Vidal (HV) [12] mixing rules and a reduced UNIQUAC model [13] to represent the complex phase behavior of CO<sub>2</sub>+1-heptanol system at different temperatures. According to their reported results, at the high temperatures of 411.99 and 431.54 K and low temperatures of 292.0 and 316 K the predicted equilibrium pressure and vapor phase CO<sub>2</sub> mole fraction are not accurate enough for process design.

Lee [14] and Oliver et al. [15] reported the VLE data for the CO<sub>2</sub>+1-pentanol and CO<sub>2</sub>+2-pentanol systems and Elizalde-Solis et al. [16] presented the high-pressure VLE data for CO<sub>2</sub>+1-propanol, CO<sub>2</sub>+2-propanol and CO<sub>2</sub>+1-butanol binary mixtures. However, their modeling approach does not give reliable VLE predictions at all ranges of pressures and temperatures.

The modeling by the conventional thermodynamic models requires the use of many adjusted parameters. The adjustment of these parameters is tedious and it is never certain to get the best set of parameters due to the problem of local minima [17].

Due to the shortcomings of the aforementioned models, an artificial neural network is presented for prediction of high pressure VLE of different binary mixtures of carbon dioxide and alkanols. The results obtained illustrate the possibility of an alternative modeling approach for predicting the VLE of CO<sub>2</sub>-alkanols mixtures.

### PROPOSED ARTIFICIAL NEURAL NETWORK (ANN) MODEL

A neural net consists of numbers of simple processing elements called neurons [18]. Each neuron of neural network is connected to others by means of a direct communication link, each with an associated weight, which represents information being used by the net to solve the problem as shown in Fig. 1. The artificial neurons are arranged in layers wherein the input layer receives inputs ( $u_i$ ) and each succeeding layer receives weighted outputs ( $w_{ij}u_i$ ) from the preceding layer as its input, resulting therefore, in a feedforward ANN, in which each input is fed forward to its succeeding layer where it is treated. The outputs of the last layer ( $v_k$ ) are real physical parameters [19,20].

A neuron in the hidden layer sums the weighted inputs from  $n$  connections plus a bias value ( $b_{ij}$ ) to produce an internal activity signal  $a_j^h$  (for neuron  $j$  of the hidden layer)

<sup>†</sup>To whom correspondence should be addressed.  
E-mail: zarenezhad@yahoo.com

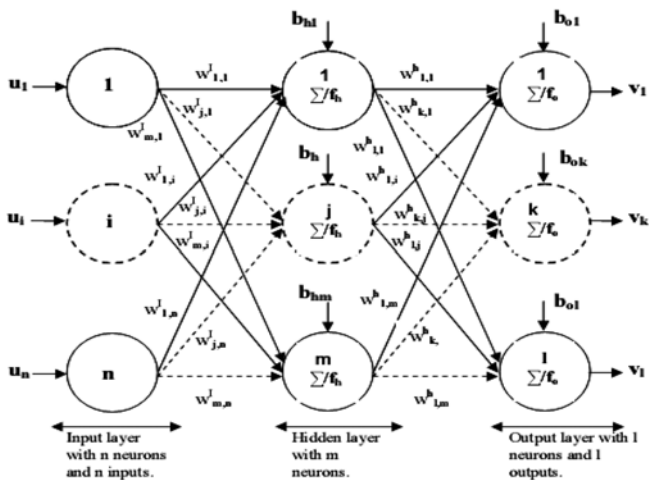


Fig. 1. Schematic diagram of a feedforward neural network model.

$$a_j^h = \sum_{i=1}^n w_{ji}^I u_i + b_{hj} \quad (1)$$

and then applies a transfer function to the sum

$$z_j = f_h(a_j^h) = f_h\left(\sum_{i=1}^n w_{ji}^I u_i + b_{hj}\right) \quad (2)$$

Where  $j=1, 2, \dots, m$ ,  $z_j$ =output of the  $j$ th neuron,  $f_h$ =activation or transfer function applied to the hidden layer,  $b_{hj}$ =bias of the  $j$ th neuron,  $w_{ji}$ =synaptic weight corresponding to  $i$ th synapse of  $j$ th neuron,  $u_i$ = $i$ th input signal to the input layer;  $n$ =number of input signals to the input layer.

The resulting signal from Eq. (2) propagates through outgoing connections to the neurons of the succeeding layer where it undergoes a similar process (for instance outputs  $z_j$  of the hidden layer fed to neuron  $k$  of the output layer gives the outputs  $v_k$ ) such that:

$$a_k^o = \sum_{j=1}^m w_{kj}^h z_j + b_{ok} \quad (3)$$

Where  $a_k^o$  is an internal activity signal (for neuron  $k$  of the output layer). Finally, we have:

$$v_k = f_o(a_k^o) = f_o\left(\sum_{j=1}^m w_{kj}^h z_j + b_{ok}\right) \quad (4)$$

Where;  $k=1, 2, \dots, l$ ,  $b_{ok}$ =bias of the  $k$ th neuron  $t$  the output layer and  $f_o$ =activation function applied to the output layer. Combining Eqs. (1) and (2) the relation between the output  $v_k$  and the inputs  $u_i$  of the neural network is obtained:

$$v_k = f_o\left(\sum_{j=1}^m w_{kj}^h f_h\left(\sum_{i=1}^n w_{ji}^I u_i + b_{hj}\right) + b_{ok}\right) \quad (5)$$

The activation function serves mainly as a type of filter or gate that lets some signals move forward and stops others as they progress from the input nodes to the output nodes. Thus, the smaller the value of the neuron's output is, the less its effect on the next neurons would be. In this work the hyperbolic tangent sigmoid activation function is used for the hidden layer, which can be written in the following

form:

$$f_h(a_j^h) = \frac{e^{a_j^h} - e^{-a_j^h}}{e^{a_j^h} + e^{-a_j^h}} \quad (6)$$

For the output layer, a linear activation function is used:

$$f_o(a_k^o) = a_k^o \quad (7)$$

The number of neurons in the input and output layers is determined by the number of independent and dependent variables, respectively. The user defines the number of hidden layers and the number of neurons in each hidden layer. Model development is achieved by a process of training in which a set of experimental data of the independent variables are presented to the input layer of the network [18-20]. The outputs from the output layer comprise a prediction of the dependant variables of the model. The network learns the relationships between the independent and dependent variables by iterative comparison of the predicted outputs and experimental outputs and subsequent adjustment of the weight matrix and bias vector of each layer by a back propagation training algorithm. Hence, the network develops a model capable of predicting with acceptable accuracy the output variables lying within the model space defined by the training set. Consequently, the objective of ANN modeling is to minimize the prediction errors of validation data presented to the network after completion of the training step.

In this work, the Levenberg-Marquardt back propagation algorithm [20] is used for network training. The training performance index  $F(w)$  to be minimized is defined as the sum of squared errors between the target outputs and the network's simulated outputs:

$$F(w) = e^T(w)e(w) \quad (8)$$

where  $w$  is the set of all network weights,  $e$  is the error vector comprising the error for all the training examples. When training with the Levenberg-Marquardt method, the weights are corrected by using the following recurrence formula:

$$w_{s+1} = w_s - (J_s^T J_s + \lambda I)^{-1} J_s^T e_s \quad (9)$$

Where the Jacobian matrix  $J$  contains the first derivatives of the network errors with respect to weights and biases, and  $\lambda$  is the learning rate. The weights correction continues until the training error function,  $F(w)$ , approaches to a minimum.

To predict the VLE of  $\text{CO}_2$ -alkanols mixtures by the proposed ANN model, the input data to the network were taken from different sources [6,9,10,14-16]. The equilibrium temperature, the  $\text{CO}_2$  mole fraction in the liquid phase, the physical properties of each pure alkanols (critical pressure, critical temperature and acentric factor) were selected as input variables, while the equilibrium pressure and the  $\text{CO}_2$  mole fraction in the vapor phase were selected as output variables. Experimental data sets were chosen with temperature range from 313.15 to 443.46 K and the pressure range from 1.14 to 21.391 MPa respectively. The experimental data used for training and generalization of ANN model are those reported by Elizalde-Solis et al. [6] for  $\text{CO}_2$ +1-hexanol and  $\text{CO}_2$ +1-heptanol systems and by Secuijanu et al. [9,10] for  $\text{CO}_2$ +1-heptanol system. Silva-Oliver et al. [15] reported the VLE of for the  $\text{CO}_2$ +1-pentanol and  $\text{CO}_2$ +2-pentanol systems. Also, Lee et al. [14] reported the VLE data for the binary mixture of  $\text{CO}_2$ +2-pentanol. Elizalde-Solis et al. [16] presented the high-pressure vapor-liquid equilibria of

**Table 1. The ranges of experimental conditions regarding different binary systems covered in this study**

System	Temperature range (K)	Pressure range (MPa)
CO <sub>2</sub> +1-Propanol	344.82-426.68	10.6-15.80
CO <sub>2</sub> +2-Propanol	334.04-443.46	2.03-13.80
CO <sub>2</sub> +1-Butanol	354.06-430.25	2.07-16.20
CO <sub>2</sub> +1-Pentanol	333.08-426.86	3.57-18.64
CO <sub>2</sub> +2-Pentanol	332.10-431.78	2.12-15.73
CO <sub>2</sub> +1-Hexanol	324.56-432.45	2.27-20.13
CO <sub>2</sub> +1-Heptanol	313.15-431.54	1.14-21.40

CO<sub>2</sub>+1-propanol, CO<sub>2</sub>+2-propanol and CO<sub>2</sub>+1-butanol binary systems. The temperature and pressure ranges of different CO<sub>2</sub>-alkanols systems used in this work are listed in Table 1.

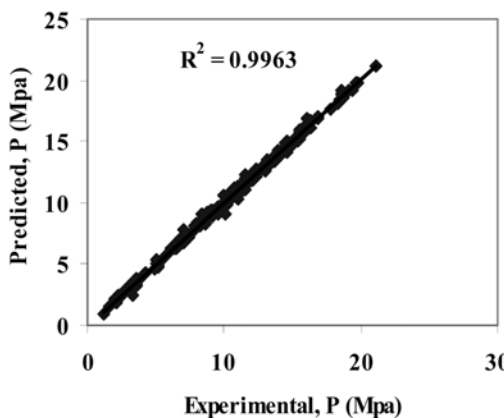
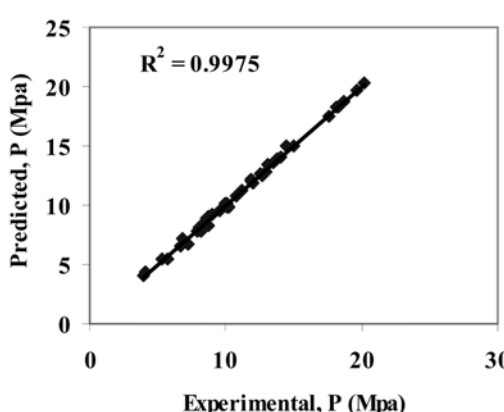
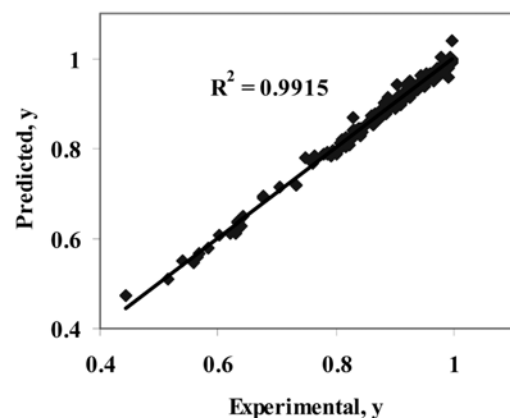
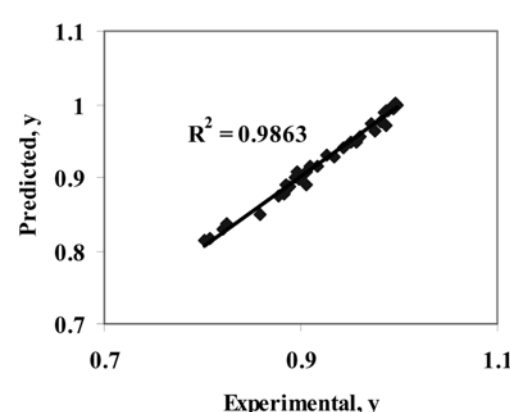
The network was trained, validated and tested by using 70%, 15% and 15% of all experimental data points, respectively. The set of data has been used to develop the neuromorphic model. A trial-and-error approach was used to minimize the error function (Eq. (8)) in order to determine the optimal combination of number of hidden layers and number of neurons. The minimum mean square error in validation test occurs when four hidden layers with 17, 14, 19 and 6 neurons in the first, second, third and fourth hidden layers are tried, respectively. The number of neurons in the input and output layers

are 5 and 2, respectively. The presented optimal network architecture can be used for predicting P (equilibrium pressure) and y (mole fraction) as a function of T (equilibrium temperature), x (mole fraction in the liquid phase), T<sub>c</sub> (critical temperature of an alkanol), P<sub>c</sub> (critical pressure of an alkanol) and  $\omega$  (acentric factor of an alkanol).

## RESULTS AND DISCUSSION

The training, validation and testing results of the proposed feed-forward neural network are displayed in Figs. 2-4. As shown, there is a very good agreement between the experimental data and the trained ones regarding equilibrium pressure (P) and vapor phase CO<sub>2</sub> mole fraction (y). The correlation coefficients ( $R^2$ -value) of the trained, validated and tested equilibrium pressure data are 0.9963, 0.9975 and 0.9978, respectively, as shown in Figs. 2-4. Also, the  $R^2$ -value of the trained, validated and tested vapor mole fraction data are 0.9915, 0.9863 and 0.9824, respectively, suggesting that the proposed network is an optimum neuromorphic structure for CO<sub>2</sub>-alkanols VLE predictions.

Figs. 5-11 show the P-x-y predictions of the proposed ANN model in comparison with the experimental data of different binary systems namely CO<sub>2</sub>+1-propanol at 373.16, 397.48 and 426.68 K; CO<sub>2</sub>+2-propanol at 344.23, 413.45 and 443.46 K; CO<sub>2</sub>+1-Butanol at 354.06, 398.98 and 430.25 K; CO<sub>2</sub>+1-Pentanol at 353.93, 374.93 and 426.86 K; CO<sub>2</sub>+2-Pentanol at 332.1, 374.15 and 431.78 K; CO<sub>2</sub>

**Fig. 2. Trained versus experimental data.****Fig. 3. Validated versus experimental data.**

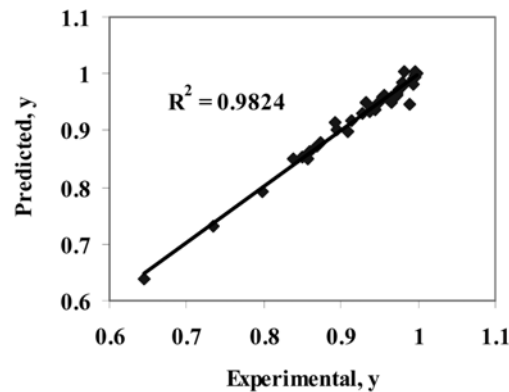
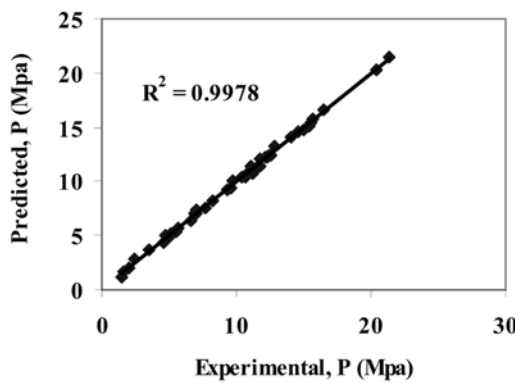


Fig. 4. Tested versus experimental data.

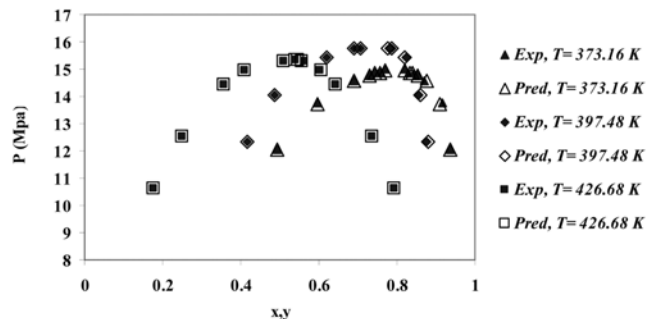


Fig. 5. Comparison of the proposed ANN model predictions with the experimental data regarding  $\text{CO}_2+1\text{-propanol}$  system.

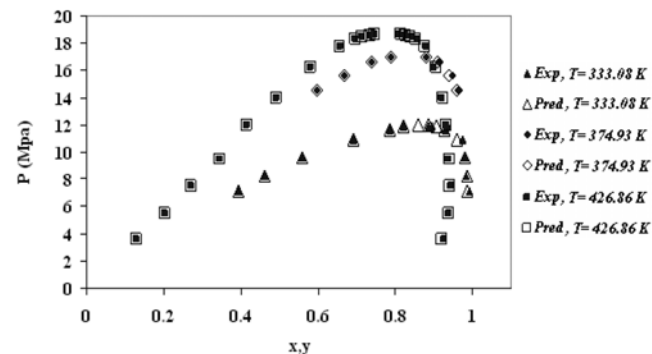


Fig. 8. Comparison of the proposed ANN model predictions with the experimental data regarding  $\text{CO}_2+1\text{-pentanol}$  system.

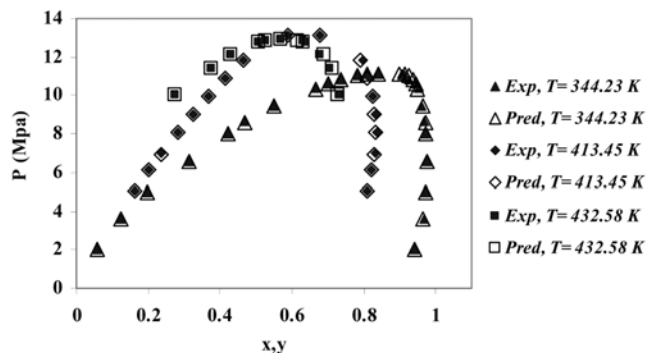


Fig. 6. Comparison of the proposed ANN model predictions with the experimental data regarding  $\text{CO}_2+2\text{-propanol}$  system.

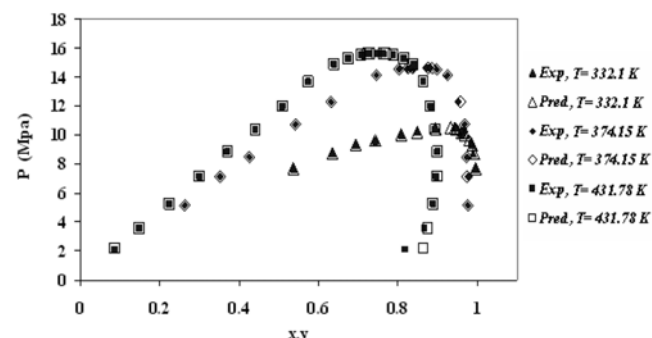


Fig. 9. Comparison of the proposed ANN model predictions with the experimental data regarding  $\text{CO}_2+2\text{-pentanol}$  system.

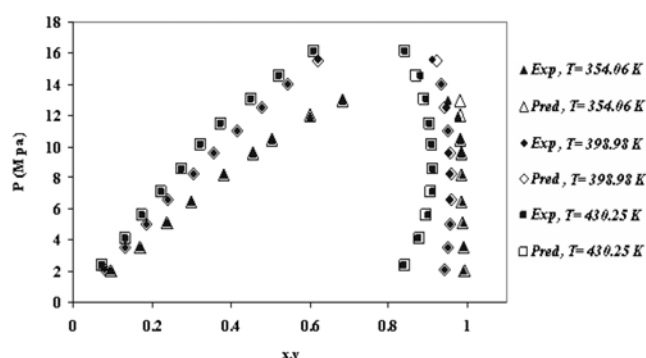
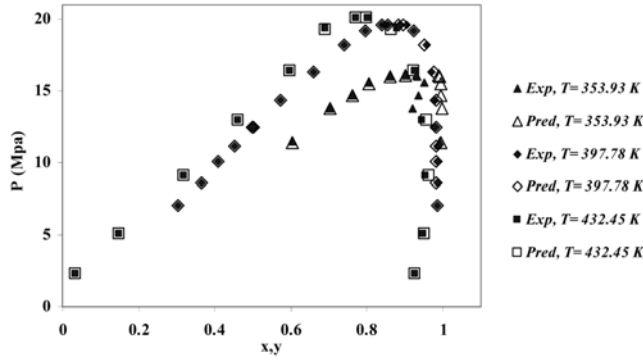


Fig. 7. Comparison of the proposed ANN model predictions with the experimental data regarding  $\text{CO}_2+1\text{-butanol}$  system.

+1-Hexanol at 353.93, 397.78 and 432.45 K and  $\text{CO}_2+1\text{-Heptanol}$  at 313.15, 374.63 and 431.54 K, respectively. As shown in these figures the predicted results are in good agreement with the measured data for all experimental systems covered in this study.

Table 2 represents the comparison between proposed ANN model predictions and SRK EOS (coupled with Huron-Vidal (HV) mixing rules and reduced UNIQUAC model) regarding  $\text{CO}_2+1\text{-heptanol}$  system. It should be noted that Elizalde-Solis et al. [6] obtained poor VLE predictions regarding  $\text{CO}_2+1\text{-heptanol}$  system by using the PR-EOS coupled with the Wong-Sandler mixing rules. As shown in Table 2, the average absolute deviations in equilibrium pressures predictions (AADP%)



**Fig. 10.** Comparison of the proposed ANN model predictions with the experimental data regarding  $\text{CO}_2+1\text{-hexanol}$  system.

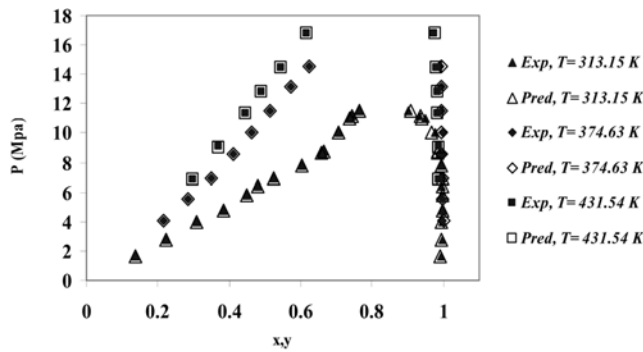


**Fig. 11.** Comparison of the proposed ANN model predictions with the experimental data regarding  $\text{CO}_2+1\text{-heptanol}$  system.

**Table 2.** Comparison between the ANN results and prediction results by SRK-HV-UNIQUAC EOS regarding the  $\text{CO}_2+1\text{-heptanol}$

T (K)	AADP% (SRK)	AADP% (ANN)	AADy% (SRK)	AADy% (ANN)
316.15	5.9	0.104	1.7	1.142
333.15	3.2	0.127	0.4	0.14
353.15	5.8	0.163	0.1	0.081
374.63	12.6	0.034	0.5	0.191
411.99	14.4	0.006	3.2	0.171
431.54	20	0.019	1.7	0.128

$$\text{AADP\%} = \frac{100}{N_p} \sum_{ip=1}^{N_p} \left| \frac{P_{ip}^{\text{exp}} - P_{ip}^{\text{pred}}}{P_{ip}^{\text{exp}}} \right| \quad (10)$$

and the average absolute deviations in the vapor phase  $\text{CO}_2$  compositions predictions (AADy%)

$$\text{AADy\%} = \frac{100}{N_y} \sum_{iy=1}^{N_y} \left| \frac{y_{iy}^{\text{exp}} - y_{iy}^{\text{pred}}}{y_{iy}^{\text{exp}}} \right| \quad (11)$$

using the presented neural network are much lower than those predicted by the SRK/HV/UNIQUAC model at different equilibrium temperatures.

The SRK-HV-UNIQUAC model predictions are compared with the proposed neural network model regarding  $\text{CO}_2+1\text{-heptanol}$  experimental data at 374.63 and 431.54 K in Figs. 12 and 13. ADP% (ab-

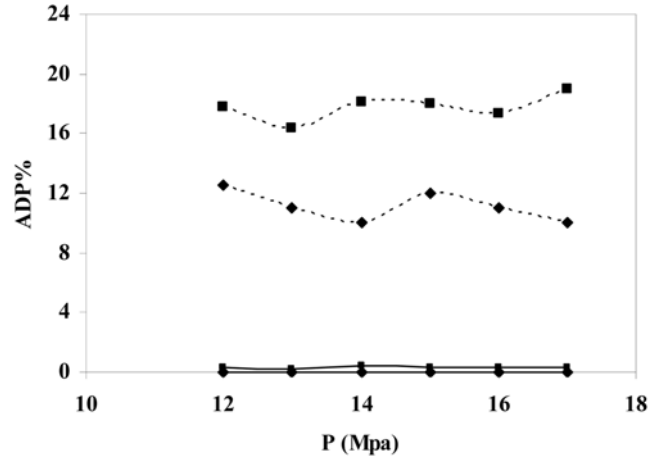


**Fig. 12.** Comparison of the proposed Neural Network (—) and SRK-HV-UNIQUAC (---) models with experimental equilibrium pressures at two different temperatures (◆ T=374.63 K and ■ T=431.54 K) regarding  $\text{CO}_2+1\text{-heptanol}$  system.

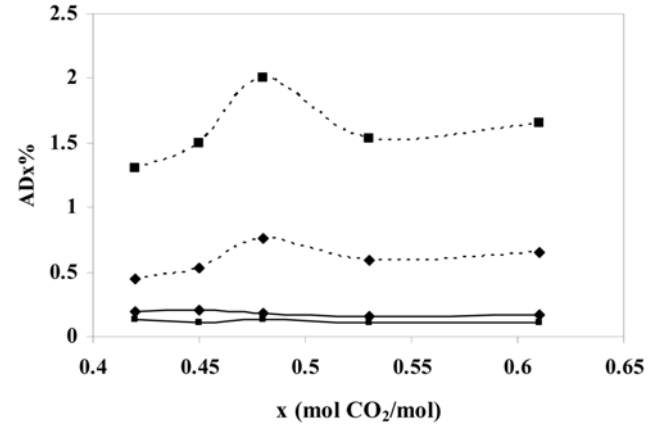


**Fig. 13.** Comparison of the proposed Neural Network (—) and SRK-HV-UNIQUAC (---) models with experimental liquid phase  $\text{CO}_2$  mole fractions at two different temperatures (◆ T=374.63 K and ■ T=431.54 K) regarding  $\text{CO}_2+1\text{-heptanol}$  system.

solute deviation% in equilibrium pressure prediction) versus P at high range of operating pressures

$$\text{ADP\%} = 100 \left| \frac{P_{ip}^{\text{exp}} - P_{ip}^{\text{pred}}}{P_{ip}^{\text{exp}}} \right| \quad (12)$$

and ADx% (absolute deviation% in liquid phase  $\text{CO}_2$  composition prediction)

$$\text{ADx\%} = 100 \left| \frac{x_{ip}^{\text{exp}} - x_{ip}^{\text{pred}}}{x_{ip}^{\text{exp}}} \right| \quad (13)$$

were used for evaluating the prediction errors. As shown in Figs. 12 and 13, the modified SRK prediction errors regarding equilibrium pressures and  $\text{CO}_2$  liquid mole fractions are oscillatory and much higher than the predictions of the proposed neural network model.

The proposed ANN model accuracy is further evaluated by com-

**Table 3. Comparison between the ANN results and prediction results by PR-VW and PR-WS EOSs regarding three different systems**

System	T (K)	AADP% (PR-VW)	AADP% (PR-WS)	AADP% (ANN)	AADy% (PR-VW)	AADy% (PR-WS)	AADy% (ANN)
CO <sub>2</sub> +1-Propanol	344.82	31.1	1.6	0.007	0.149	0.013	0.0051
	373.16	6.2	0.7	0.014	0.077	0.006	0.0021
	397.48	4.5	1.6	0.022	0.083	0.005	0.002
	426.68	3.09	0.7	0.019	0.127	0.012	0.0035
CO <sub>2</sub> +2-Propanol	334.04	8.5	1.2	0.039	0.097	0.013	0.0073
	344.23	14.3	1.7	0.107	0.014	0.012	0.0042
	353.72	2.3	0.3	0.031	0.051	0.008	0.0100
	373.18	3.4	0.6	0.064	0.036	0.024	0.0019
	398.62	7.1	0.3	0.073	0.05	0.015	0.0064
	413.45	3	0.8	0.065	0.018	0.015	0.0022
CO <sub>2</sub> +1-Butanol	443.46	3.6	1.5	0.073	0.062	0.02	0.0125
	354.06	5.7	0.5	0.025	0.003	0.003	0.0013
	398.98	3.7	0.9	0.036	0.005	0.008	0.0024
	430.25	4.8	2.8	0.202	0.006	0.011	0.0036

**Table 4. Comparison between the ANN results and prediction results by PT-WS EOS**

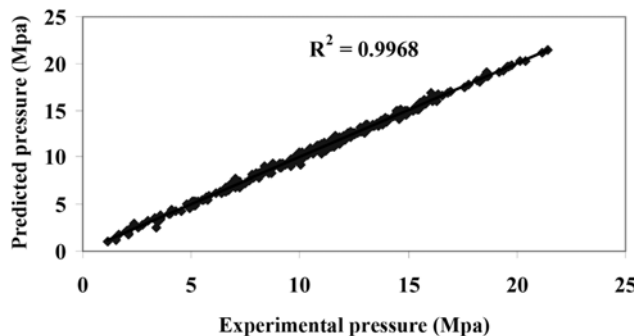
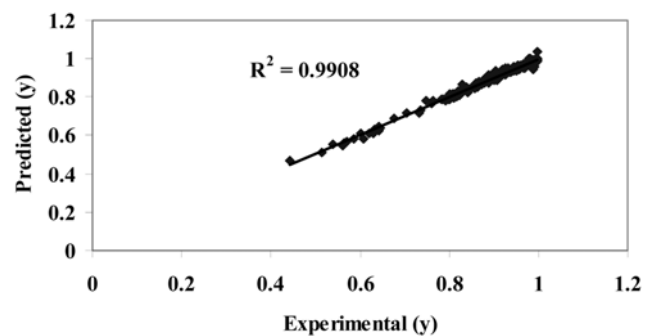
System	T (K)	AADP% (PT EOS)	AADP% (ANN)	AADy% (PT EOS)	AADy% (ANN)
CO <sub>2</sub> +1-Pentanol	343.69	1.9	0.12	5.76	1.41
	374.93	0.24	0.005	0.6	0.37
	426.86	1.1	0.11	0.52	0.39
CO <sub>2</sub> +2-Pentanol	343.61	1.14	0.02	1.32	0.31
	374.15	1.31	0.015	1.4	0.26
	397.56	0.59	0.015	0.36	0.28
	431.78	0.86	0.14	0.87	0.82

paring its predictions with those obtained through the Peng-Robinson PR EOS coupled with Van der Waals (VW) and the Wong-Sandler (WS) mixing rules regarding CO<sub>2</sub>+1-propanol, CO<sub>2</sub>+2-propanol and CO<sub>2</sub>+1-butanol systems in Table 3. As shown in Table 3, the average absolute deviations in equilibrium pressures predictions (AADP%) and the average absolute deviations in the vapor phase compositions predictions (AADy%) using the presented ANN model are always lower than those of the PR-VW and PR-WS models.

Table 4 represents the comparison between the proposed ANN model and the Patel and Teja equation of state (PT EOS) [21] coupled with WS mixing rules regarding two binary systems of CO<sub>2</sub>+1-pentanol and CO<sub>2</sub>+2-pentanol at different temperatures. As shown

in Table 4, the predictions of the proposed ANN model for estimation of the equilibrium pressure and vapor phase CO<sub>2</sub> composition are always better than those obtained through the PT EOS. To obtain a relatively good match between EOS predictions and the experimental data, it is necessary to fit the EOS mixture parameters to the VLE data at each temperature. However, in the proposed ANN model such a fitting procedure is not required.

The proposed ANN model predictions are compared with all experimental data in Figs. 14 and 15. The correlation coefficients (R<sup>2</sup>-value) for equilibrium pressure and vapor phase CO<sub>2</sub> mole fraction predictions are 0.9968 and 0.9908, respectively, indicating a very good agreement between the experimental and predicted values.

**Fig. 14. Comparison between proposed ANN model predictions and experimental equilibrium pressures.****Fig. 15. Comparison between proposed ANN model predictions and experimental vapor phase CO<sub>2</sub> mole fractions.**

As shown in these figures, the proposed feed-forward neural network model can be used for accurate prediction of CO<sub>2</sub>-Alkanol vapor-liquid equilibrium conditions and proper design of high pressure separation units.

## CONCLUSIONS

Accurate prediction of the high pressure/temperature phase behavior of CO<sub>2</sub>-alkanol mixtures, particularly in supercritical conditions, is essential for the design of separation processes. Therefore, a feed-forward neural network model with four hidden layers is developed to predict the vapor-liquid equilibrium of seven binary mixtures of CO<sub>2</sub>-alkanols. The presented model is very accurate over wide ranges of experimental pressure and temperatures. The correlation coefficient (R<sup>2</sup>-value) for equilibrium pressure and vapor phase CO<sub>2</sub> mole fraction predictions are 0.9968 and 0.9908, respectively, indicating a very good agreement between the experimental and predicted values. Comparison of the suggested neural network model with the most important thermodynamic correlations shows that the proposed nuromorphic model outperforms the other available alternatives.

## ACKNOWLEDGEMENT

The second author would like to thank the office of gifted students of Semnan University for its financial support.

## NOMENCLATURE

T	: equilibrium temperature [K]
T <sub>c</sub>	: critical temperature of an alkanol [K]
P	: equilibrium pressure [MPa]
P <sub>c</sub>	: critical pressure of an alkanol [MPa]
y	: mole fraction of CO <sub>2</sub> in the vapor phase
x	: mole fraction of CO <sub>2</sub> in liquid phase
N <sub>p</sub>	: number of equilibrium pressure data points
N <sub>y</sub>	: number of vapor phase CO <sub>2</sub> composition data points
AADP%	: percent of average absolute deviation in predicting the equilibrium pressure
ADP%	: absolute deviation percent in pressure prediction
AADy%	: percent of average absolute deviation in predicting the vapor composition
ADx%	: absolute deviation percent in prediction of liquid CO <sub>2</sub> mole fraction
R <sup>2</sup> -value	: correlation coefficient
z <sub>j</sub>	: output of the jth neuron
f <sub>h</sub>	: activation function applied to the hidden layer
f <sub>o</sub>	: activation function applied to the output layer
b <sub>hj</sub>	: bias of the jth neuron in the hidden layer
b <sub>ok</sub>	: bias of the kth neuron in the output layer
w <sup>I</sup> <sub>ji</sub>	: synaptic weight corresponding to ith synapse of jth neuron
w <sup>h</sup> <sub>kj</sub>	: synaptic weight corresponding to jth synapse of kth neuron
u <sub>i</sub>	: ith input to the input layer
v <sub>k</sub>	: kth output of the output layer
h	: hidden layer
o	: output layer
n	: number of input layer neurons
m	: number of hidden layer neurons

<i>l</i>	: number of output layer neurons
i	: neuron i in the input layer
ip	: index of the component ip
j	: neuron j in the hidden layer
k	: neuron k in the output layer
F	: error function
J	: Jacobian matrix
$\lambda$	: learning rate
s	: iteration number
e	: the error vector
I	: identity matrix
T	: transpose of a matrix
a <sup>h</sup> <sub>j</sub>	: an internal activity signal (for neuron j of the hidden layer)
a <sup>o</sup> <sub>k</sub>	: an internal activity signal (for neuron k of the output layer)
$\omega$	: acentric factor
exp	: experimental
pred	: predicted

## REFERENCES

- E. J. Beckman, *J. Supercrit. Fluids*, **28**, 121 (2004).
- S. N. Joung, C. W. Yoo, H. Y. Shin, S. Y. Kim, K. P. Yoo and C. S. Lee, *Fluid Phase Equil.*, **185**, 219 (2001).
- CRC Handbook of Chemistry and Physics, 89<sup>th</sup> Ed., CRC Publishing, USA (2008).
- H. Orbey and S. I. Sandler, *Modeling vapor-liquid equilibria: Cubic equations of state and their mixing rules*, Cambridge Univ. Press, Cambridge (1998).
- M. Castier, L. A. Galicia-Luna and S. I. Sandler, *Braz. J. Chem. Eng.*, **21** (2004).
- O. Elizalde-Solis, L. A. Galicia-Luna, S. I. Sandler and J. G. Samayo-Hernández, *Fluid Phase Equilib.*, **210**, 215 (2003).
- D. Y. Peng and D. B. Robinson, *Ind. Eng. Chem. Fund.*, **15**, 59 (1976).
- D. S. H. Wong and S. I. Sandler, *AIChE J.*, **38**, 671 (1992).
- C. Secuiyanu, V. Feroiu and D. Geană, *Fluid Phase Equilib.*, **261**, 337 (2007).
- C. Secuiyanu, V. Feroiu and D. Geană, *Fluid Phase Equilib.*, **270**, 109 (2008).
- G. Soave, *Chem. Eng. Sci.*, **27**, 1197 (1972).
- M. Huron and J. Vidal, *Fluid Phase Equilib.*, **3**, 255 (1979).
- B. Wisniewska-Gocłowska and S. K. Malanowski, *Fluid Phase Equilib.*, **180**, 103 (2001).
- H.-S. Lee and H. Lee, *Fluid Phase Equilib.*, **695**, 150 (1998).
- G. Silva-Olivier, L. A. Galicia-Luna and S. I. Sandler, *Fluid Phase Equilib.*, **200**, 161 (2002).
- O. Elizalde-Solis, L. A. Galicia-Luna and L. E. Camacho-Camacho, *Fluid Phase Equilib.*, **259**, 23 (2007).
- V. H. Alvarez, R. Larico, Y. Ianos and M. Aznar, *Braz. J. Chem. Eng.*, **25** (2008).
- P. R. B. Guimaraes and C. McGreavy, *Comput. Chem. Eng.*, **19**, 741 (1995).
- D. Graupe, *Principles of Artificial Neural Networks*, 2<sup>nd</sup> Ed., WSPC, USA (2007).
- P. G. Benardos and G-C. Vosniakos, *Engineering Applications of Artificial Intelligence*, **20**, 365 (2007).
- N. C. Patel and A. S. Teja, *Chem. Eng. Sci.*, **37**, 463 (1982).